

CHAPTER 188

PRACTICAL APPLICATION OF THE THREE-DIMENSIONAL BEACH EVOLUTION MODEL

Takuzo Shimizu¹, Hitoshi Nodani² and Kosuke Kondo³

ABSTRACT

The long-term bottom topography changes around the entrance of a fishery harbour were simulated by using the three-dimensional beach evolution model. The practical applicability of the model was demonstrated through comparisons with the actual topographical changes. And the equilibrium state of beach evolution due to construction of a coastal structure could be also predicted by repeating the calculation of the wave and current field and that of the bottom topography change.

1. INTRODUCTION

In constructing a harbour on a sandy coast, it is necessary to give careful consideration not only to countermeasures against sand deposition at the entrance of or inside the harbour, but also to the effects on the neighbouring beaches. So, the beach evolution due to construction of a coastal structure must be predicted in order to design a suitable layout plan of breakwaters.

In recent years, a numerical simulation model of beach evolution, so-called a three-dimensional beach evolution model, has been rapidly developed and applied to many practical problems in Japan, since Watanabe et al.(1986) proposed a model and confirmed its validity on the basis of laboratory experimental data. However, quantitative verification of its applicability to the actual field has not been thoroughly discussed.

In this study, we aimed to discuss quantitatively, through comparisons with field data, the applicability of the model to the long-term topographical changes around Iiooka Fishery Harbour, Chiba, Japan.

¹Senior Engineer, Design and Engineering Department,

²Engineer, Design and Engineering Department,

³Divisional Manager, Research and Development Department, Penta-Ocean Construction Co.,Ltd. 2-2-8 Koraku, Bunkyo-ku, Tokyo 112, Japan.

2. OUTLINE OF THE MODEL

The numerical simulation model used in this study is fundamentally similar to the model proposed by Watanabe et al. (1986). Figure 1 shows the calculation flow of the model. The total model consists of three submodels for calculation of waves, nearshore currents and beach changes. At the first step, the wave field is computed under a certain incident wave condition and the initial bottom topography in the study area. Next, the nearshore current field is computed from the spatial distribution of radiation stresses which is estimated by using the results of the wave field computation. Finally, the sediment transport rates are computed at the local points from the wave-current conditions calculated in advance, and then the three-dimensional bottom topography change is computed by solving the equation of sediment mass conservation.

The incident wave conditions change daily and the change in bottom topography produce changes in the nearshore waves and currents. So, the short time-interval iterations are needed in the computations of waves, currents and topography changes. In practice, the iterations using daily wave conditions are not possible, because the computation time of each model is not sufficiently short. But only one step of the iteration is useful to predict the tendency of the spatial distribution of bottom topography change under a representative wave condition. This way of application of the model is effective to discuss relatively the merits or demerits of layout of breakwaters.

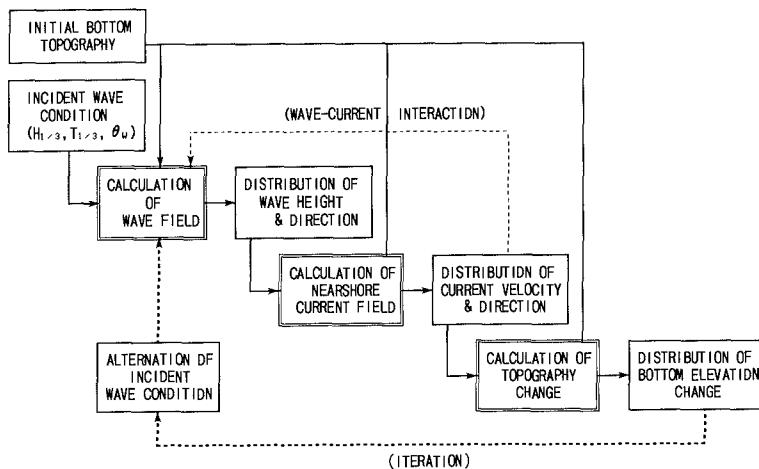


Fig.1 Flow chart of computation

On the other hand, in order to quantitatively predict the long-term beach evolution due to construction of the coastal structures, the interaction between the wave and current field and the bottom topography change cannot be ignored and several iterations are needed. So, we attempted to reduce the number of iterations by using a simply modelled series of wave conditions.

Table 1 shows the calculation methods of waves, currents and beach changes. The wave field is computed using the energy flux equation as described with the directional wave spectrum presented by Karlsson(1969). The wave heights in the surf zone are estimated by the model of random wave breaking proposed by Goda(1975). This equation is applicable only for wave shoaling and refraction, and is not for wave diffraction in a strict sense. Recently, more accurate equations for combined refraction and diffraction such as the mild-slope equation and its approximate parabolic-type equations are often adopted. Watanabe and Maruyama(1986) also presented the time-dependent mild-slope equations. These are applicable to calculate all kinds of wave transformation including wave breaking as well as shoaling, refraction and diffraction. But the applicability of the computation models based on these equations are generally restricted to the linear regular wave. The reason for using the method based on the energy flux equation is because treatment of random waves is important for practical applications and because the computing time of the actual random wave field in a wide region is relatively short.

In computing the nearshore current field, the spatial distributions of radiation stresses were estimated as regular waves; the wave energy and the principal direction at the local point were estimated from the directional wave spectrum calculated in the wave field computation, and the group velocity and the wave celerity were estimated by using the significant wave period.

As the momentum exchange coefficient, the expression proposed by Longuet-Higgins(1970) was adopted. The mixing length is generally set to be the distance from the shoreline, but in this study, it was set to be the shortest length either from the breakwater or from the shoreline. Then, the nearshore current field including circulation near the breakwater could be reproduced better.

In calculating bottom elevation change, we employed the formula of local sediment transport rate in a wave-current coexistent field proposed by Watanabe et al.(1986). This model is simple and practical. The sediment transport rate is divided into the transport due

to mean currents and that due to waves. The cross-shore sediment transport rate due to waves is assumed to be important to the short-term beach deformation, and not so important to the long-term change. In many cases, sediment transport due to nearshore currents is the dominant feature of long-term change caused by construction of a coastal structure. So, in this study, only the sediment transport due to nearshore currents were taken into account. The local sediment transport rates were evaluated using the quantities corresponding to the significant wave and the principal direction.

Table 1 Calculation methods of three submodels

CALCULATION OF WAVE FIELD
(REFRACTION) Wave energy flux equation (Karlsson, 1969) (BREAKING) Goda's model (1975) (DIFFRACTION) Energy flux transmitted from the breakwater is zero
CALCULATION OF NEARSHORE CURRENT FIELD
Vertically integrated equations of mean momentum and of continuity
CALCULATION OF BOTTOM ELEVATION CHANGE
Equation of sediment mass conservation [Local sediment transport rate formula proposed by Watanabe et al. (1986)] Sediment transport due to mean currents q_c : $q_c = A_c (\tau - \tau_c) u_c / \rho g$ where A_c : a non-dimensional coefficient, τ : the maximum value of the bottom shear stress in a wave and current coexistent field, τ_c : the critical shear stress for the onset of sediment movement, u_c : the mean current velocity.

3. PRACTICAL APPLICATION OF THE MODEL

3.1 TOPOGRAPHY CHANGES AROUND IIOKA FISHERY HARBOUR

Figure 2 shows the location map of Iioka Fishery Harbour. Iioka Fishery Harbour faces directly to the Pacific Ocean and is located at the northeastern end of the Kujyukuri Coast. This coast is one of the most famous sandy beaches with the continuous coastline of 55km and bounded at both ends by eroding sea cliffs. The northern sea cliff, Byobugaura, stretches northeastward 10km long and is bordered immediately on the north by Iioka Fishery Harbour. And the Byobugaura Cliff has supplied considerable amounts of sediment to the Kujyukuri Coast.

Judging from an aerial photograph taken in February of 1986 shown in Photo 1, it was a little stormy day with the significant wave height of about 2m. Looking at the crestlines of waves, we will find that the incident wave attacks the harbour much obliquely and then the longshore drift to the southwest is predominant.

As Iioka Fishery Harbour is located at the passing point of longshore drift from the Byobugaura Cliff to the Kujyukuri Coast, a large portion of longshore sand drift has been obstructed by the harbour. Consequently, not only harbour shoaling but also beach erosion of the neighbouring beaches have occurred.

Figure 3 shows the bottom topography change around the harbour during approximately one and half years from June of 1986 to November of 1987. The upper figure shows the comparison of bottom contours and the lower shows the distribution of depth changes. Considerable accretion took place along the breakwater on the updrift side of the harbour, especially around the entrance. On the other hand, erosion took place on the downdrift side. The mechanism of these beach deformations can be explained by the following two kinds of nearshore currents. One is the longshore current developing westward on the eastern side of the harbour, and another is the clock-wise nearshore circulation in the sheltered area of the breakwater on the western side. This is a typical case of beach deformation in constructing a structure on a sandy coast with considerable amounts of longshore drift.

3.2 VERIFICATION OF THE WAVE AND CURRENT COMPUTATIONS

In order to verify the wave and current field computations, the field observation was carried out around Iioka Fishery Harbour over a period of approximately one month from September to November in

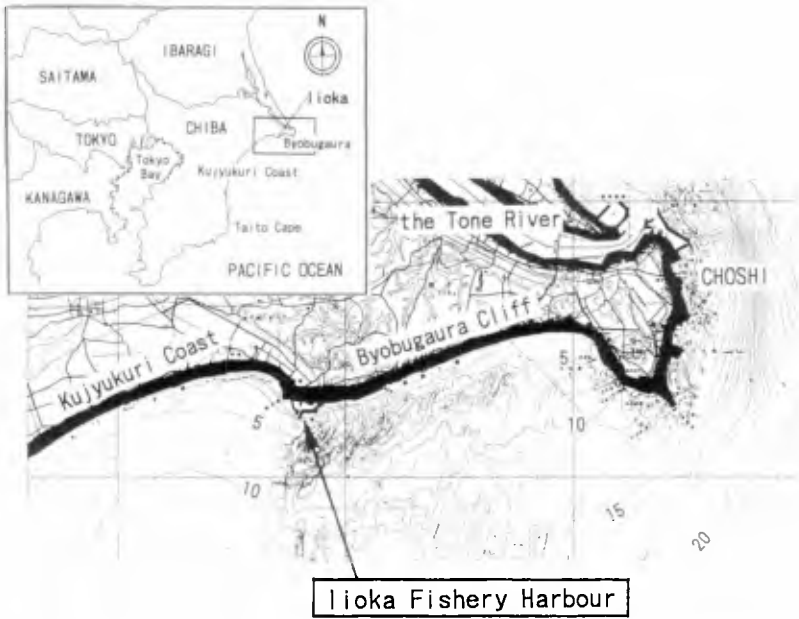


Fig.2 Location map of investigation site

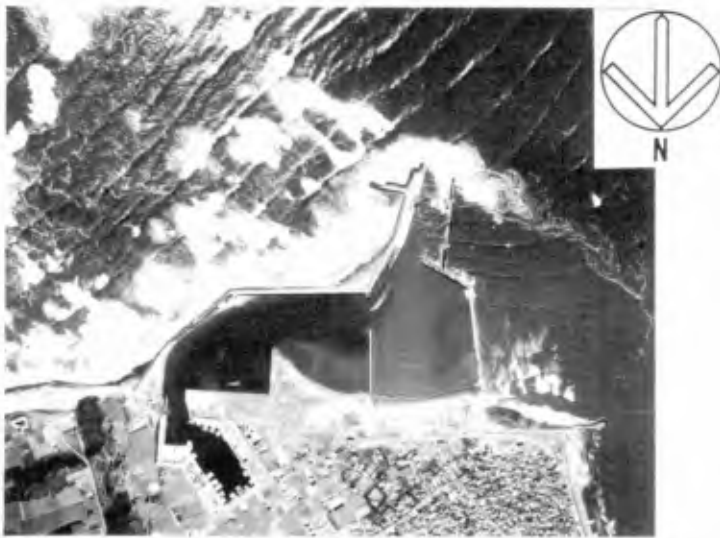
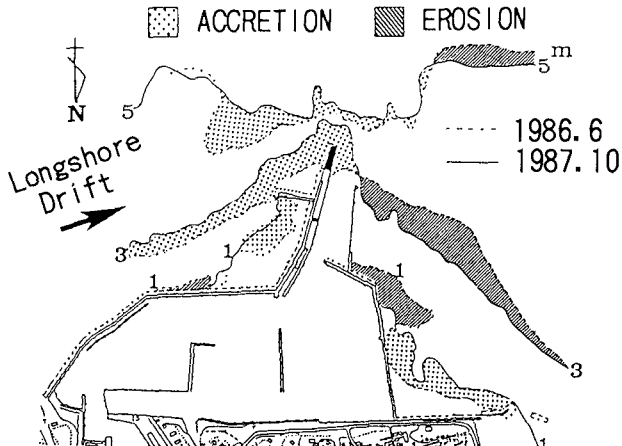
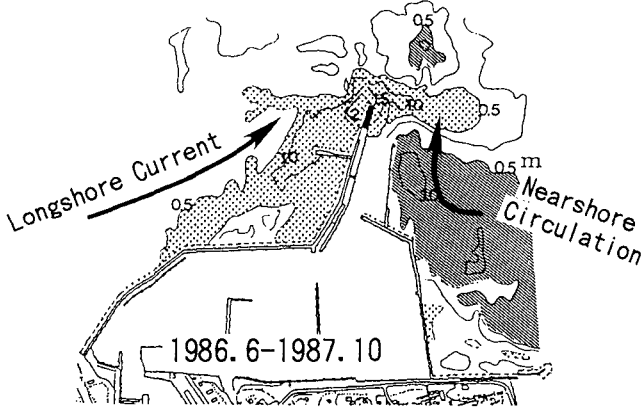


Photo 1 Aerial photograph (February, 1986)



(a) Comparison of bottom contours



(b) Distribution of depth change

Fig.3 Bottom topography change around lioka Fishery Harbour(1986.6-1987.10)

1987. Figure 4 shows the measuring points around the harbour where wave directions and nearshore currents were observed using electro-magnetic current meters. Incident wave conditions such as wave heights, periods and directions were also measured using a combination of an ultra-sonic wave gauge and an electro-magnetic current meter at a water depth of 15m offshore in front of the harbour. During the observation, storm waves greater than 2m in significant wave height were frequently encountered. Therefore, we could collect much data on the large waves caused by typhoons.

Figure 4 also shows the computation area which is about 4km long in the alongshore direction and about 6km long in cross-shore direction. Three cases of wave height conditions were treated, that is, the significant wave height of 2m with its period of 8s, 3m with 10s and 4m with 12s. With respect to these three cases of wave height conditions, three wave directions of ESE, SE and SSE were considered. And totally nine cases of computations were performed. According to these nine cases of calculations, measured data of wave directions and mean currents were divided into nine classes in total. And the mean values of wave directions and mean currents at each point in every class were regarded as the measured values and compared with the results of the computations.

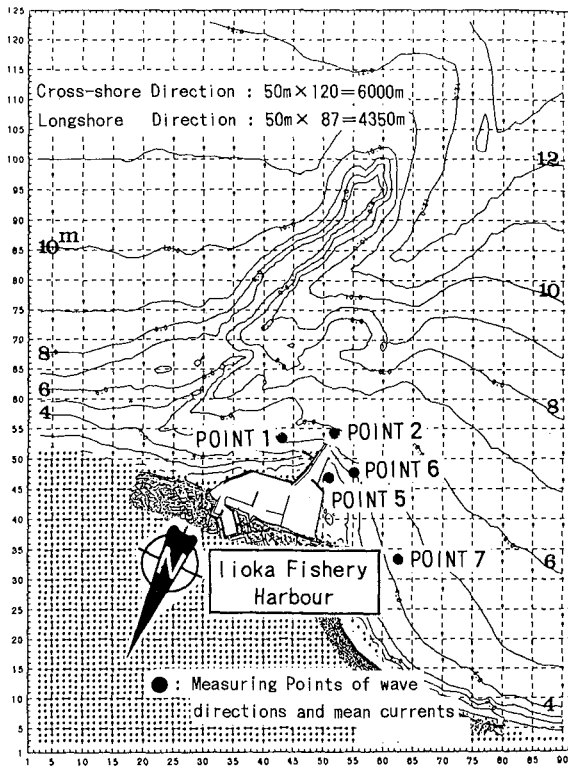


Fig.4 Location of the current meters and the area of numerical simulation

Figure 5 shows comparisons between the measured and the computed principal wave directions. As the wave propagating directions are scarcely affected by the incident wave periods in the range of 8 to 12 seconds, the results of computations of 3m in wave height with 10 seconds in wave period were used. The computed results show fairly good agreement with the observed.

Figure 6 shows the examples of the nearshore current computations under the wave direction of ESE. The measured vectors are also shown in this figure and expressed by bold arrows in the different scale from the calculated vectors. The longshore current develops westward along the eastern breakwater and passes the entrance of the harbour quickly. And the clock-wise circulation occurs remarkably around the western side of the harbour entrance. The observed dominant current pattern is reproduced satisfactorily by the numerical simulation.

Figure 7 shows comparisons between measured and computed absolute values and directions of mean current vectors. The computed results are compared with only reliable data which satisfy such conditions that the current velocity is beyond 5 cm/s and the current direction is stable. There exists a little disagreement between the measured and the calculated. However, in spite of assuming the quasi-stationary wave and current field and neglecting the wave-current interaction, the computed results agree well with the measurements, especially at the POINT 2 in front of the harbour entrance.

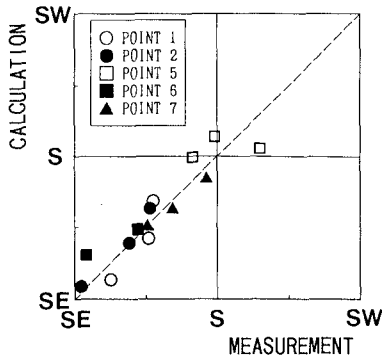


Fig.5 Comparison between the measured and the calculated principal wave direction

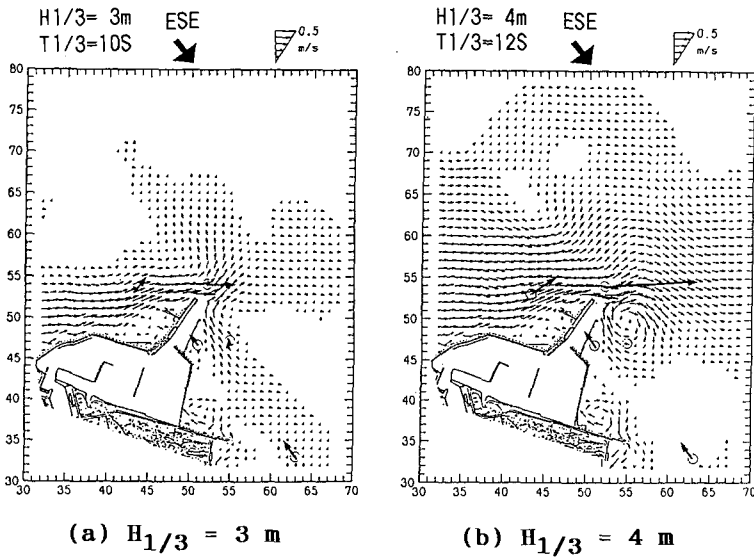


Fig. 6 Distribution of the calculated nearshore current field and the measured current vectors

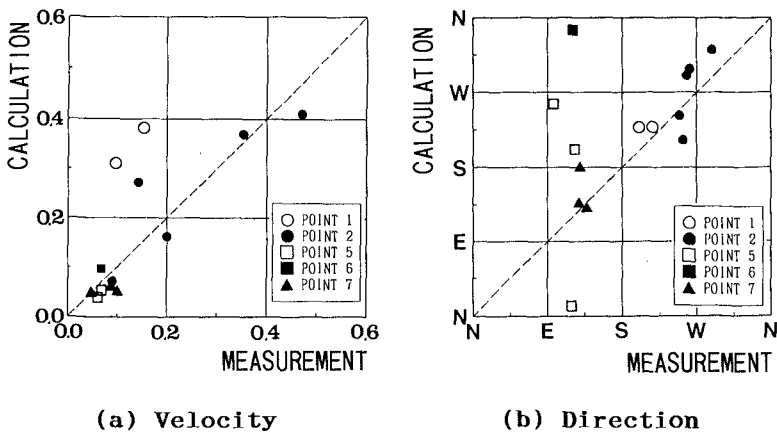


Fig. 7 Comparison between the measured and the calculated velocities and directions of the nearshore current

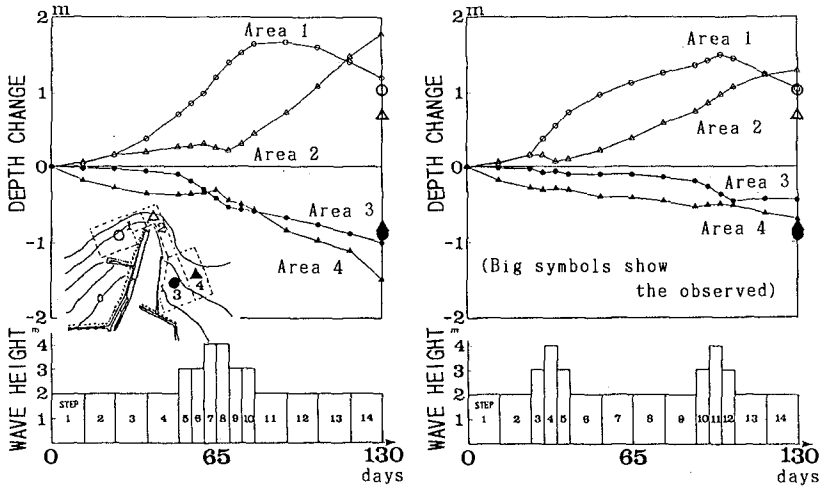
3.3 REPRODUCTION OF THE LONG-TERM BEACH EVOLUTION

We tried to reproduce quantitatively the long-term topography changes around Ilioka Fishery Harbour during approximately one and half years shown in Figure 3. The numerical simulation was performed by repeating the calculation of the wave-current field and that of the beach changes alternatively. In order to shorten the computation time, we attempted to use the three modelled wave conditions. These have one, two, or four series of severe waves for the investigation period of one and half years (peak significant wave height is 4m). The occurrence frequency of severe waves was determined on the basis of the observed wave climate data, and each modelled wave condition has the same occurrence frequency in total. The wave conditions with the significant wave height below 2m were not taken into account, because the longshore current could not reach the entrance of the harbour and little accretion took place under such a calm wave condition.

Figure 8 shows the calculated time series of mean depth variations in the four areas around the harbour entrance. In every case, the calculated depth variations after one and half years (130 days of severe waves) show accretion of about 1.0m in Area 1 and 2, and erosion of about 0.5m in Area 3 and 4. These results agreed quantitatively with the actual topographical changes.

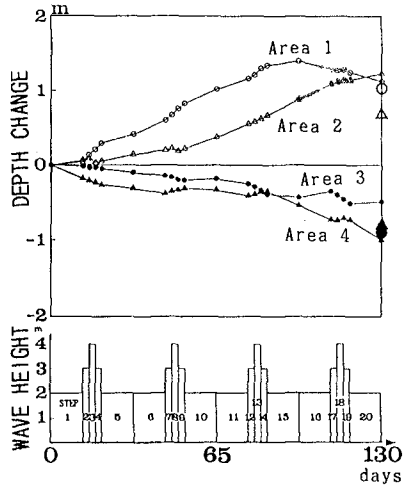
Investigating more precisely the results of case 2, in Area 1 along the breakwater on the updrift side, rapid accretion takes place during the first severe wave series. And the depth change reaches an equilibrium state after the first severe wave series. In Area 2 at the harbour entrance, rapid accretion takes place after accretion advanced in Area 1, and the depth change then reaches an equilibrium after the second severe wave series. On the other hand, in case 1, an equilibrium state is not reached in Area 2 after only one series of severe waves.

Figure 9 shows comparisons between the measured and the computed bottom elevation changes. Big symbols indicate the average in each area and small symbols indicate the values at each calculation grid. Although there exist a little disagreement at the local points, the averaged value of calculation in each area shows good agreement with that of observation. In spite of greatly simplifying the wave conditions, it is found that the long-term beach evolution around the harbour entrance and its consequent bottom topography change can be reasonably simulated by using a model with two or more series of severe waves.



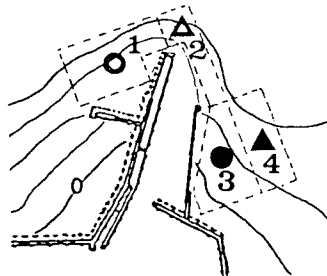
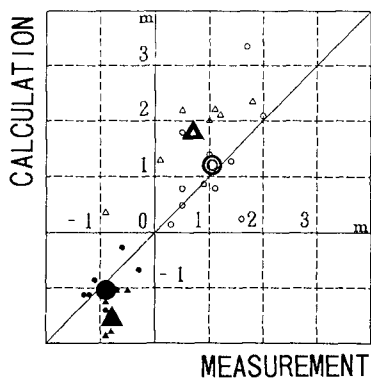
(a) Case 1

(b) Case 2

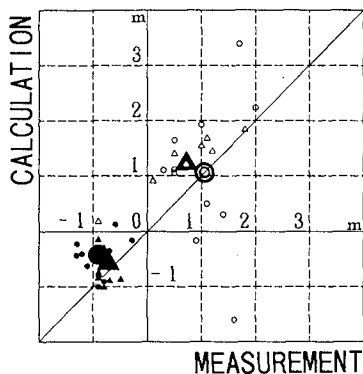


(c) Case 3

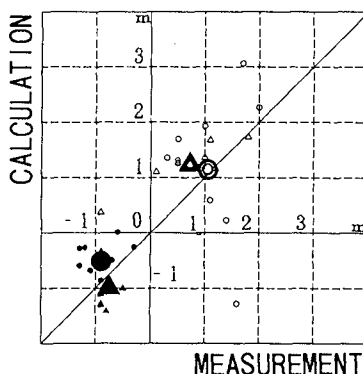
Fig. 8 Comparison between the measured and the calculated bottom elevation changes



(a) Case 1



(b) Case 2



(c) Case 3

Fig.9 Calculated time series of depth changes in the four areas around the harbour

4. CONCLUSIONS

The bottom topography change around a fishery harbour during one and half years were simulated by using the three-dimensional beach evolution model under the simplified wave condition. It is concluded that the model has the required accuracy for practical use and that the equilibrium state of topography change can be also predicted.

ACKNOWLEDGMENTS

We would like to express our thanks to Dr. Yamamoto of National Research Institute of Fisheries Engineering and Mr. Nishi of the Japanese Institute of Technology on Fishing Ports and Communities (now, Fisheries Agency) for their advice and useful discussion.

REFERENCES

- Goda, Y. (1985): Irregular wave deformation in the surf zone, Coastal Eng. in Japan, Vol.18, pp.13-26.
- Karlsson, T. (1969): Refraction of continuous ocean wave spectra, Proc. ASCE, Vol.95, No. WW4, pp.437-448.
- Longuet-Higgins, M.S. (1970): Longshore currents generated by obliquely incident sea waves, Jour. of Geophys. Res., Vol.75, No.33, pp.6778-6789.
- Watanabe, A., K. Maruyama, T. Shimizu and T. Sakakiyama (1986): Numerical prediction model of three-dimensional beach deformation around a structure, Coastal Eng. in Japan, Vol.29, pp.179-194.
- Watanabe, A. and K. Maruyama (1986): Numerical modeling of nearshore wave field under combined refraction, diffraction and breaking, Coastal Eng. in Japan, Vol.29, pp.19-40.